

Explanatory and Illustrative Visualization of Special and General Relativity

Daniel Weiskopf, *Member, IEEE Computer Society*, Marc Borchers,
 Thomas Ertl, *Member, IEEE Computer Society*, Martin Falk, Oliver Fechtig, Regine Frank,
 Frank Grave, Andreas King, Ute Kraus, Thomas Müller, Hans-Peter Nollert, Isabel Rica Mendez,
 Hanns Ruder, Tobias Schafhitzel, Sonja Schär, Corvin Zahn, and Michael Zatloukal

Abstract—This paper describes methods for explanatory and illustrative visualizations used to communicate aspects of Einstein's theories of special and general relativity, their geometric structure, and of the related fields of cosmology and astrophysics. Our illustrations target a general audience of laypersons interested in relativity. We discuss visualization strategies, motivated by physics education and the didactics of mathematics, and describe what kind of visualization methods have proven to be useful for different types of media, such as still images in popular science magazines, film contributions to TV shows, oral presentations, or interactive museum installations. Our primary approach is to adopt an egocentric point of view: The recipients of a visualization participate in a visually enriched thought experiment that allows them to experience or explore a relativistic scenario. In addition, we often combine egocentric visualizations with more abstract illustrations based on an outside view in order to provide several presentations of the same phenomenon. Although our visualization tools often build upon existing methods and implementations, the underlying techniques have been improved by several novel technical contributions like image-based special relativistic rendering on GPUs, special relativistic 4D ray tracing for accelerating scene objects, an extension of general relativistic ray tracing to manifolds described by multiple charts, GPU-based interactive visualization of gravitational light deflection, as well as planetary terrain rendering. The usefulness and effectiveness of our visualizations are demonstrated by reporting on experiences with, and feedback from, recipients of visualizations and collaborators.

Index Terms—Visualization, explanatory computer graphics, illustrative visualization, special relativity, general relativity, astrophysics, visualization of mathematics, terrain rendering.

1 INTRODUCTION

ALBERT Einstein (1879-1955) was the first truly international pop star of science, and his popularity has never been matched by any other scientist since. In part, his popularity is certainly due to his extraordinary personality, appearance, and political engagement. Even more importantly, though, special and general relativity are concerned with concepts that everybody experiences in daily life, such as space, time, and light—at the same time engendering an aura of scientific complexity and paradoxical effects. Therefore, most people are both attracted to and appalled

by Einstein's theories, which show that properties of space, time, and light in relativistic physics are dramatically different from those of our familiar environment governed by classical physics.

A major and typical problem in explaining special and general relativity to nonphysicists is a lack of mathematical background, especially in differential geometry. We strongly believe that visualization can be used to address this problem because it is an excellent means of conveying important aspects of Einstein's theories without the need for mathematical formalism. Our goal is to develop visualizations that are explanatory, illustrative, and pedagogical in nature. Our approach does not target data exploration, but the communication of ideas, theories, and phenomena to others. Although data and information exploration is the focus of most research efforts in the visualization community, we think that visual communication is an equally important aspect of visualization. Relativistic and astrophysical visualization is heavily based on mathematics, physics, and computer graphics and, therefore, is rooted in the tradition of scientific visualization.

We have shown a long-term commitment for relativistic visualization, with our group having started related research at the end of the 1980s [1], [2]. Over the years, we have been improving technical methods and didactical approaches for relativistic visualization. This paper reports on our experiences and it also contributes technical descriptions of algorithms. Our experiences are based on numerous visualization projects such as accompanying illustrations for

- D. Weiskopf is with the Graphics, Visualization, and Usability Lab, School of Computing Science, Simon Fraser University, Burnaby, BC V5A 1S6, Canada. E-mail: weiskopf@cs.sfu.ca.
- M. Borchers, O. Fechtig, R. Frank, F. Grave, A. King, U. Kraus, T. Müller, H.-P. Nollert, I. Rica Mendez, H. Ruder, C. Zahn, and M. Zatloukal are with the Institute for Astronomy and Astrophysics, University of Tübingen, Auf der Morgenstelle 10, 72076 Tübingen, Germany. E-mail: {borchers, fechtig, frank, boot, aking, kraus, tmueller, nollert, isabel, ruder, zahn, zatloukal}@tat.physik.uni-tuebingen.de.
- T. Ertl, M. Falk, and T. Schafhitzel are with the Institute of Visualization and Interactive Systems, University of Stuttgart, Universitätsstr. 38, 70569 Stuttgart, Germany. E-mail: {ertl, schafhitzel}@vis.uni-stuttgart.de, falkmn@studi.informatik.uni-stuttgart.de.
- S. Schär is with the Historisches Museum Bern, Helvetiaplatz 5, 3005 Bern, Switzerland. E-mail: sonja.schaer@gmx.net.

Manuscript received 14 Nov. 2005; revised 17 Jan. 2006; accepted 25 Jan. 2006; published online 10 May 2006.

For information on obtaining reprints of this article, please send e-mail to: tcvg@computer.org, and reference IEEECS Log Number TVCGSI-ERTL-1105.

popular science articles in magazines and book chapters, animated visualizations for TV shows, as well as technical and scientific contents for major exhibitions. These different types of media and presentational forms require different methods, equipment, workflows, and know-how. Therefore, we are an interdisciplinary team of 15-20 people with expertise in computer graphics, relativistic physics, physics education, visual perception, user interfaces, computer-based modeling and animation, as well as museum design. Moreover, this team collaborates with journalists and writers in the context of popular science publications. In particular, our visualizations have been widely used in the context of popular science presentations for the Einstein year 2005—the 100th anniversary of Einstein’s *annus mirabilis*, in which he published his seminal articles on Brownian motion, the photoelectric effect, and special relativity. Nevertheless, we have also been experiencing a continuing significant demand for relativistic visualization independent of a specific anniversary.

This paper discusses our strategies for explanatory visualization as well as technical issues of algorithms, implementations, and workflows. We present how and why we employ different methods and tools, and we describe technical contributions in the form of extended or novel visualization methods for image-based special relativistic rendering on GPUs (graphics processing units), special relativistic 4D ray tracing for accelerating scene objects, general relativistic ray tracing for spacetimes with non-trivial topology, GPU-based interactive visualization of gravitational light deflection, and realistic planetary terrain rendering.

This paper extends our previous work [3], which focuses on our experiences with relativistic and astrophysical visualization for a general audience. In this paper, we additionally discuss technical aspects and algorithms in more detail, including those for special relativistic rendering (Section 3) and general relativistic rendering (Section 4). Furthermore, we extend our previous discussion of more abstract visualizations of relativistic light propagation and curved space (Section 5) and we show how these types of visualization can be combined with special and general relativistic rendering.

For a comprehensive presentation of related work on relativistic visualization, we refer to Black [4], who provides detailed descriptions and a chronologically ordered list of published and unpublished (Web-based) previous work, and to the list of published references given by Weiskopf [5]. Where needed, directly related previous work is referenced throughout this paper.

2 VISUALIZATION STRATEGIES

In general, visualizations contain both explicit and implicit information [6], [7]. A mismatch between facts implicit in the visualization and those implicit in the theory or the data results in two types of problems. The visualization is not *complete* if not all facts implied by the theory are also implied by the visualization. Incomplete visualizations do not need to be incorrect. In fact, incompleteness is a valid means of reducing complexity and is frequently used in our visualizations in order to decrease the cognitive load for the

user. Conversely, a visualization is not *sound* if it implies facts that are not valid consequences of the theory or data. Unfortunately, many popular science presentations of relativity contain visualizations that are misleading, not sound, or even completely wrong.

We address the issue of soundness by relying on a visualization metaphor that is easy to explain and that avoids unnecessary implications: A virtual experiment is conducted under the influence of relativistic effects and the images taken by a virtual camera are the basis for the visualization, i.e., an egocentric view is adopted in a visually enriched thought experiment [8]. For example, special relativistic effects can be demonstrated by virtual flights at a velocity close to the speed of light or general relativity can be illustrated by viewing a virtual galaxy behind a black hole that acts as source for gravitational light bending. The idea is to construct instructive, interesting, and compelling scenarios, e.g., with high-speed travel, black holes, wormholes, or the large scales covered by cosmology.

Our approach has several advantages. First, the underlying scenario can be easily described to a layperson. Second, the concept of a real or virtual camera is well-known from cinema, TV, or computer games. Third, image generation corresponds to a physical experiment that simulates light propagation. Therefore, the fundamental issue of coordinate system dependency, inherent to general relativity, is automatically addressed [9]. We apply the egocentric strategy for special relativity (Section 3), general relativity (Section 4), and cosmological flights (Section 6). The strategy also lends itself to the intentional use of incompleteness: Separate relativistic effects on light propagation can be selectively switched on or off, e.g., color changes due to Doppler shift may be switched off to focus on geometric effects only.

An alternative strategy is based on the tradition of mathematical visualization. In general, this strategy tends to rely on more abstract metaphors that are more difficult to explain and that may be misleading. Therefore, an exocentric mathematical visualization of relativity has to be carefully designed from a didactical point of view. Section 5 describes our approaches for the exocentric illustrations of relativistic light propagation and curved geometry. We often use an abstract exocentric visualization in combination with the egocentric visualization of the same phenomenon because such a linking of different points of views can promote a more thorough understanding, while it helps to avoid the implications of an unsound presentation.

3 SPECIAL RELATIVISTIC RENDERING

The mathematical foundation of special and general relativity is built on the concept of 4D spacetime, i.e., the combination of 3D space and 1D time. Special relativity is able to describe the kinematics of photons, which have vanishing rest mass, and massive objects alike. General relativity is only required when gravitation needs to be included (see Section 4). Special relativistic effects become noticeable at velocities comparable to the speed of light. Therefore, our approach to special relativistic visualization is based on virtual motion at very high speed.

3.1 Object-Space Approach for Special Relativistic Rendering

Special relativity is based on flat spacetime, described by the Minkowski metric [10], [11]. Points in spacetime, so-called events, are transformed between reference frames moving at different velocities by the Lorentz transformation. The Lorentz transformation of light emission events is the basis for an object-space approach to special relativistic rendering [12]. For relativistic motion in a static scene, object-space rendering boils down to a nonlinear transformation of spatial positions from the static scene to spatial positions as seen by the fast moving camera.

For interactive rendering, this transformation is first applied to the vertices of the scene objects, and then the transformed geometry is rendered by usual methods of nonrelativistic computer graphics. This object-space approach nicely fits to the GPU rendering pipeline: Vertex coordinates are modified at the first stage of the rendering pipeline, whereas the other stages of the pipeline remain unaffected. The vertex transformation can be computed in a vertex shader program, which makes the implementation transparent to all other parts of the rendering software (see, e.g., the implementation from one of our undergraduate students' projects¹). While object-space relativistic rendering is easy to implement and fast, it may suffer from quality problems: The nonlinear transformations of vertex coordinates are incompatible with the linear connections between vertices through straight edges. These artifacts are most prominent for large and close-by triangles. The solution is a fine and ideally view-dependent retessellation of the scene, which, however, implies significant changes and extensions to the implementation of the rendering pipeline.

3.2 Image-Based Approach for Special Relativistic Rendering

More recently, we have developed image-based special relativistic rendering [13] as an alternative rendering method that only requires computations in 2D image space. It builds upon the concept of the plenoptic function $P(\mathbf{x}, \theta, \phi, \lambda)$, which describes the radiance of the light depending on direction (θ, ϕ) in spherical coordinates, spacetime position \mathbf{x} , and wavelength λ [14]. The basic idea is to first record the plenoptic function within a static scene and for a static camera and then to transform the plenoptic function into the frame of a moving camera. Afterward, nonrelativistic rendering methods can be applied to construct the final image.

The Lorentz transformation of the plenoptic function is determined by three relativistic effects: relativistic aberration of light, Doppler effect, and searchlight effect. The relativistic aberration of light causes a modification of the direction of light and is able to describe the apparent geometry seen by a fast moving camera. The Doppler effect accounts for the transformation of wavelength and causes a change in color. The searchlight effect transforms radiance and, e.g., increases the brightness of objects ahead when the observer is approaching these objects at high velocity.

Let us consider two inertial frames of reference, S and S' , with S' moving with velocity v along the z axis of S . A light ray is described by direction (θ, ϕ) and wavelength λ in

frame S and by (θ', ϕ') and λ' in frame S' . Then, the Lorentz transformation of the plenoptic function from S to S' is [13]

$$P'(\theta', \phi', \lambda') = D^{-5} P\left(\arccos \frac{\cos \theta' + \beta}{1 + \beta \cos \theta'}, \phi', \frac{\lambda'}{D}\right), \quad (1)$$

with the Doppler factor $D = \gamma(1 + \beta \cos \theta')$, $\gamma = 1/\sqrt{1 - \beta^2}$, $\beta = v/c$, and the speed of light c . The plenoptic functions P and P' are located at corresponding spacetime positions, which are no longer explicitly shown in the mathematical expressions.

A direct application of image-based special relativistic rendering is used to transform real-world images [13]. Real images are most useful in illustrating relativistic effects in our familiar environment: They provide a "before-and-after" effect applied to our everyday world and therefore facilitate an easy recognition of relativistic effects affecting well-known scenes. An important technical problem is that aberration leads to severe distortions in image space that require the acquisition of high-resolution input images with a very large field of view—usually, even a full spherical panorama (i.e., with 4π solid angle) is needed. Data acquisition is time-consuming for a single panorama and extremely difficult for flights based on a series of several hundred panoramas. Even if a collection of panorama images were available, storage and real-time processing of the data would be challenging, making an interactive rendering of relativistic motion very difficult. Therefore, we use real-world image-based rendering only for pre-computed illustrations—either for still images in magazines, or in films for exhibitions and TV shows.

The Lorentz transformation of the plenoptic function can also be applied to synthetic images. The basic idea is to construct a panorama by rendering a virtual scene and then to transform this panorama. The following kinds of functionality play a key role in an efficient GPU implementation. First, cube maps can be used to store a panorama. Second, cube maps can be efficiently constructed by render-to-texture functionality. Third, and most importantly, the Lorentz transformation from (1) can be implemented by GPU fragment programs.

Our implementation of image-based special relativistic rendering is based on C++ and OpenGL. Aberration of light is realized with a dependent texture read from the synthetic cube map, implemented by a few fragment program instructions. Depending on the simulated velocity and the resulting distortion, different combinations of supersampling and filtering are used to achieve high image quality. The Doppler and searchlight effects are implemented using precomputed textures as lookup tables for the transformed colors of different materials in the scene.

Based on our experience, we have decided to exclusively use image-based rendering as the basis for interactive special relativistic visualization. The advantages of image-based rendering are: First, almost the same rendering pipeline can be used as for nonrelativistic rendering. Unmodified nonrelativistic rendering is used to fill the panorama cube maps; the subsequent Lorentz transformation is just one additional rendering step. In particular, image-based rendering does not interfere with the core rendering routines and the scene representation, while object-space rendering needs a view-dependent retessellation of the scene to avoid artifacts from nonlinear transformations of vertex coordinates. Second, illumination

1. http://www.vis.uni-stuttgart.de/relativity/sr_viewer.



Fig. 1. Special relativistic visualization of apparent geometry at $\beta = 0.95$.

computations, based on the Doppler and searchlight effects, can be readily included. Third, image-based rendering is per-pixel accurate, both for geometric and illumination effects. Fig. 1 shows an example for the image-based visualization of geometric effects for an observer traveling with 95 percent of the speed of light. For this scene, our GPU implementation achieves some 90-125 fps (frames per second) for the visualization of apparent geometry and some 60 fps for the visualization of geometric and illumination effects on an ATI Radeon X800 XT GPU.

3.3 Four-Dimensional Special Relativistic Ray Tracing

Standard nonrelativistic ray tracing is performed in 3D space and one may think of relativistic ray tracing as ray tracing in 4D spacetime. While this is true for the general case, the special situation of static scenes can be handled by ray tracing in three dimensions. In fact, the early ray-tracing method by Hsiung and Dunn [15] is based on traditional 3D ray tracing enriched by a transformation of primary ray directions from the moving camera frame to the frame of the static scene.

We usually do not employ 3D ray tracing for special relativistic rendering because it is restricted to static scenes, which can be handled by image-based rendering more efficiently. However, ray tracing is useful for visualizing a wider range of phenomena, including accelerating scene objects as well as shadowing, reflection, or transmission of light. Full 4D special relativistic ray tracing is needed to allow for these effects and it requires the following extensions:

First, a 3D ray is replaced by a straight ray in four dimensions, i.e., the starting point and the direction of the ray have one temporal and three spatial coordinates. Second, the ray projector has to generate 4D rays. The 4D starting position and time as well as the spatial direction of a ray are known from the camera parameters. Third, the scene objects have to be linked to their motion through spacetime, i.e., they have to store their spatial and temporal positions for the complete time span of an animation. The intersection between light rays and objects is computed in 4D spacetime. The intersections correspond to emission, absorption, or transmission events. Fourth, in order to calculate local illumination for an intersection event at an object, the direction of the light ray and the spectral power distribution that is transported along the light ray have to be transformed to the reference frame of the respective object. This transformation is accomplished according to (1). In the case of an accelerating scene object, a

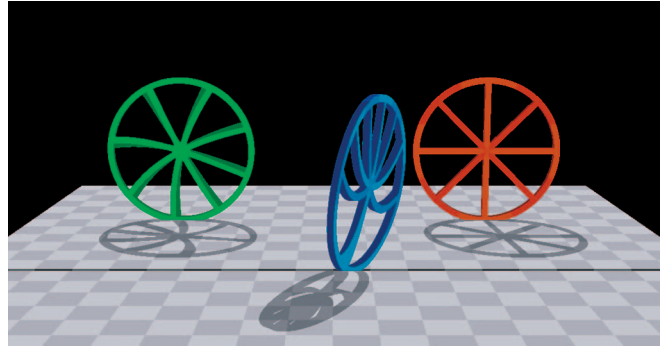


Fig. 2. Special relativistic visualization of moving and rotating wheels. © 2002 C. Zahn.

comoving inertial frame of reference is used to determine the kinetic parameters for the Lorentz transformation.

In our implementation, the spatial shape and motion of an object are not separated, but tightly linked and stored together in the scene graph. In this way, the world line—the spacetime path—of an object is encoded. Our approach, in particular, is capable of describing inertial and accelerated motion alike, i.e., it supports straight and curved world lines. This support for arbitrary motion is one aspect that distinguishes our approach from the framework by Li et al. [16], who, e.g., provide illustrations of relativistic reflection and transmission phenomena.

Fig. 2 shows an example of 4D special relativistic ray tracing. The scene consists of a ground surface with a checkerboard pattern at rest. The red wheel is also at rest. The green wheel rotates clockwise in place in a way that a point on the outer perimeter moves with $\beta = 0.93$. The blue wheel rolls with a speed of $\beta = 0.93$ from left to right along the thin horizontal line, i.e., it undergoes rotational and translational motion simultaneously. Note that the blue wheel is oriented parallel to the other two wheels. The scene is illuminated by directional light from above and behind the scene. Fig. 2 demonstrates the effect of the finite speed of light, e.g., in the form of the shadows cast by the green and blue wheels: The total distance from a point on the wheel to the shadow point on the ground surface and then to the camera is longer than the distance between the wheel and the camera. Due to the finite speed of light, the shadow has to correspond to an earlier position of the wheel than the image of the wheel itself. In addition, Fig. 2 shows that the flexibility of having accelerated scene objects is very useful because rotation is a typical example for noninertial motion. In order to emphasize the effects of the Lorentz contraction and the finite speed of light, this visualization only shows the apparent geometry of moving objects, neglecting the Doppler and searchlight effects.

Four-dimensional ray tracing is slightly slower than nonrelativistic 3D ray tracing due to the additional operations for the Lorentz transformation of light and the more complex computation of intersections between light rays and objects in 4D spacetime. Therefore, we use ray tracing only for precomputed images and films, e.g., for still images in popular science publications or electronic films on Web pages.

3.4 Interaction Methods for Special Relativistic Motion

Although images and movies give a good impression of relativistic motion, an improved impression is achieved

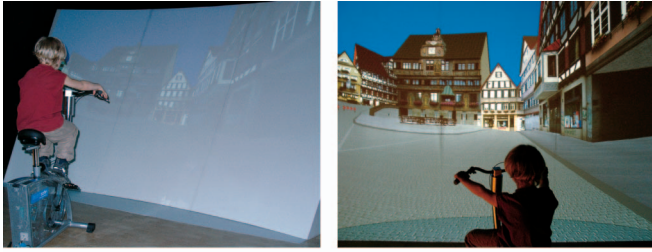


Fig. 3. Interactive special relativistic visualization. Users can control their motion by a bicycle interface.

through interactive exploration of a relativistic scenario. As outlined in Section 3.2, we use image-based rendering for interactive special relativistic visualization.

In an interactive session, users are allowed to steer their high-speed motion through a static scene, including acceleration of the camera. As basis for navigation and camera control, the relativistic-vehicle-control metaphor [17] is adopted—an extension of the nonrelativistic flying-vehicle or virtual-camera metaphors. The user can control the direction and velocity of motion with a joystick (for smaller installations or desktop environments) or a bicycle interface, which is useful for large-screen installations. Fig. 3 shows an example from an exhibition in the “Stadthaus” in Ulm (March 2004–August 2004). From experience, the bicycle interface is very intuitive for visitors of exhibitions because it provides a good and expected mapping between controls and their effects: This interface exploits functional mimicry because relativistic navigation imitates real-world navigation on a bicycle [18]. Our installation for Ulm allowed the user to navigate through a highly detailed 3D model of Tübingen that was originally designed for the Virtual Tübingen project [19] by the Max Planck Institute for Biocybernetics, Tübingen. Another exhibition, at the “Historisches Museum” in Bern (June 2005–October 2006), uses a 3D model of Bern, showing Einstein’s commuting route to his workplace at the patent office. The Bern model was specifically designed for the exhibition by our collaborators at the “Historisches Museum” in Bern.

4 GENERAL RELATIVISTIC RENDERING

General relativity extends special relativity to include gravitation. Through gravitational sources, the flat Minkowski spacetime of special relativity becomes curved. Concepts from differential geometry are employed to describe curved spacetimes [10], [20]. A basic concept of differential geometry is the line element

$$ds^2 = \sum_{\mu, \nu=0}^3 g_{\mu\nu}(\mathbf{x}) dx^\mu dx^\nu,$$

where $g_{\mu\nu}(\mathbf{x})$ is an element of the 4×4 metric tensor at spacetime position \mathbf{x} and dx^μ is an infinitesimal distance in the μ direction of the coordinate system. Light travels along geodesics—the analogues to straight lines in curved spacetime. Geodesic lines can be computed as solutions to the geodesic equation,

$$\frac{d^2 x^\mu(\lambda)}{d\lambda^2} + \sum_{\nu, \rho=0}^3 \Gamma^\mu_{\nu\rho}(\mathbf{x}) \frac{dx^\nu(\lambda)}{d\lambda} \frac{dx^\rho(\lambda)}{d\lambda} = 0, \quad (2)$$

where λ is an affine parameter for the geodesic line. The Christoffel symbols $\Gamma^\mu_{\nu\rho}$ are computed from the metric:

$$\Gamma^\mu_{\nu\rho}(\mathbf{x}) = \sum_{\alpha=0}^3 \frac{g^{\mu\alpha}(\mathbf{x})}{2} \left(\frac{\partial g_{\alpha\nu}(\mathbf{x})}{\partial x^\rho} + \frac{\partial g_{\alpha\rho}(\mathbf{x})}{\partial x^\nu} - \frac{\partial g_{\nu\rho}(\mathbf{x})}{\partial x^\alpha} \right),$$

where $g^{\mu\alpha}(\mathbf{x})$ is the inverse of $g_{\mu\alpha}(\mathbf{x})$.

4.1 Single-Chart Ray Tracing

Images, as seen by a virtual camera in a general relativistic setting, can be generated by nonlinear 4D ray tracing [2], [9], [21], [22]. The starting point is a standard 3D Euclidean ray tracing, which needs three major extensions to incorporate general relativistic rendering. First, straight light rays in three dimensions have to be replaced by geodesic light rays in four dimensions, which can be approximated by polygonal lines. Second, the ray projector that generates a light ray corresponding to a pixel on the image plane has to be modified to compute light propagation governed by the geodesic equation (2). The initial value problem for this system of ordinary differential equations can be solved by numerical integration, e.g., an adaptive fourth-order Runge-Kutta method. Initial values are determined by the position, orientation, and field of view of the observer’s camera and by the coordinates of the corresponding pixel on the image plane. The third extension concerns the intersection between light rays and scene objects that has to take into account a fourth, temporal coordinate.

We allow for a local frame of the camera that can be different from the global coordinate system that describes the scene and the curved light rays. In this way, a high flexibility is achieved in controlling camera parameters. The initial values are first computed in the coordinate system of the camera, which is a local Minkowski system, and then they are transformed into the global coordinate system for actual ray tracing. For a pixel on the image plane, a corresponding direction $\hat{\mathbf{y}}$ with three space components $(\hat{y}^1, \hat{y}^2, \hat{y}^3)$ is associated, as known from nonrelativistic ray tracing. We assume that the direction vector is normalized to unit length: $\|\hat{\mathbf{y}}\| = 1$. The time coordinate \hat{y}^0 follows from the null condition for light rays, $\sum_{a,b=0}^3 \eta_{ab} \hat{y}^a \hat{y}^b = 0$, where

$$\eta_{ab} = \begin{pmatrix} -1 & 0 & 0 & 0 \\ 0 & 1 & 0 & 0 \\ 0 & 0 & 1 & 0 \\ 0 & 0 & 0 & 1 \end{pmatrix}$$

is the Minkowski metric associated with the local frame. Given the initial direction $\hat{\mathbf{y}}^\mu$ in the local frame, the corresponding initial direction y^μ of a light ray in the global reference frame follows from

$$\sum_{a=0}^3 \hat{y}^a \hat{\mathbf{e}}_{(a)} = \sum_{a,\mu=0}^3 \hat{y}^a e_a^\mu \mathbf{e}_\mu = \sum_{\mu=0}^3 y^\mu \mathbf{e}_\mu.$$

Here, a vector in the camera frame, $\hat{\mathbf{e}}_{(a)}$, and a vector in the μ direction of the global coordinate system, \mathbf{e}_μ , are related by $\hat{\mathbf{e}}_{(a)} = \sum_{\mu=0}^3 e_a^\mu \mathbf{e}_\mu$, where e_a^μ is a general linear map with $\det e_a^\mu > 0$. Furthermore, the map e_a^μ has to satisfy the orthonormality condition $\sum_{\mu,\nu=0}^3 g_{\mu\nu} e_a^\mu e_b^\nu = \eta_{ab}$.

Fig. 4 shows an example of general relativistic ray tracing: It displays a spherical surface located in the Schwarzschild spacetime [10], which describes the metric



Fig. 4. Egocentric visualization of the Schwarzschild spacetime. © 2005 D. Weiskopf.

of a nonrotating massive object. The surface texture of the Earth is applied to visualize the distortions due to light deflection. For comparison, Fig. 5 shows a corresponding exocentric view of light bending by a massive object.

4.2 Multiple-Charts Ray Tracing

So far, we have assumed a single coordinate system in which light rays are computed. In general, however, the geometry of spacetime has a nontrivial topology that can only be represented by an atlas containing several charts, i.e., several coordinate systems. A teapot with handle and pot is an example of a 2D manifold with nontrivial topology. The implementation of an atlas leads to an extension of the data structures for ray tracing. First, a light ray now consists of 5D points with four spacetime coordinates and one chart number (an ID). A light ray is decomposed in different segments that belong to different charts. In each chart, the light ray segment is determined by the geodesic equation (2), based on the associated spacetime metric. When the light ray exits one chart and enters another chart, the position and direction of the previous segment are transformed from the previous chart to the new one, yielding the initial values for the following ray segment. The concept of an atlas also affects the representation of scene objects. Each object is associated with a single chart, and ray-object intersections are computed on a chart-by-chart basis.

As another extension, we represent scene objects with respect to a local reference frame $\{\hat{\mathbf{e}}_{(a)}\}$. In this way, moving objects can be described, similarly to the motion of a camera

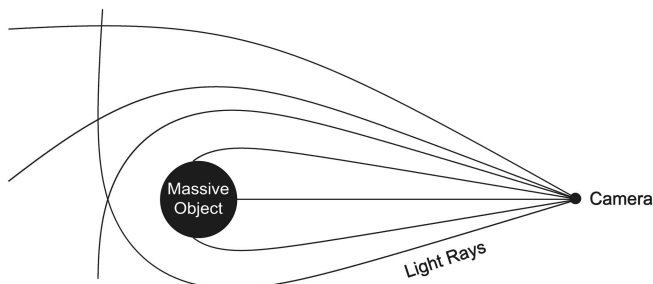


Fig. 5. Exocentric illustration of gravitational light deflection in the Schwarzschild spacetime. Light rays are shown as lines bent by a massive object.

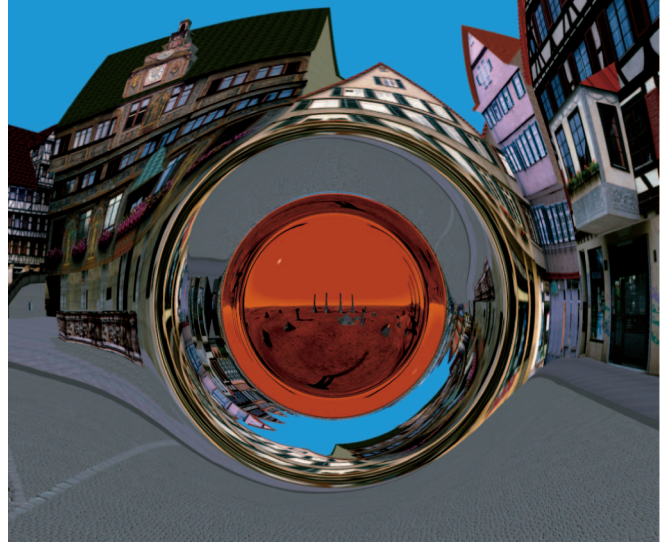


Fig. 6. Ray tracing in nontrivial topology: A wormhole between the market place of Tübingen and a fictitious Mars station. © 2005 M. Borchers and T. Müller.

described above. The position and velocity of a free-falling object is determined by the geodesic equation (2), along with the condition for the motion of any mass-like object: $\sum_{a,b=0}^3 \eta_{ab} \dot{\mathbf{y}}^a \dot{\mathbf{y}}^b = -1$. Furthermore, the vectors within the local frame undergo parallel transport, which is described by

$$\frac{dX^\mu}{d\tau} + \sum_{\nu,\rho=0}^3 \Gamma^\mu_{\nu\rho} u^\nu X^\rho = 0,$$

where X^μ is any 4D vector to be transported, u^ν is the four-velocity—a 4D description of velocity—and τ is the proper time of a comoving clock [10].

An interesting spacetime with nontrivial topology is a wormhole connecting two far-away regions of spacetime [23]. Both charts have a metric of the form

$$ds^2 = -e^{2\phi(r)} dt^2 + \frac{dr^2}{1 - b(r)/r} + r^2 (d\vartheta^2 + \sin^2 \vartheta d\varphi^2),$$

where $\phi(r)$ is the redshift-function, $b(r)$ is the shape-function, and (r, ϑ, φ) are spherical coordinates. The charts are connected by the wormhole throat, which is a 2D surface of spherical topology.

As detailed by Müller [24], a member of our research group, the ray-tracing visualization of wormholes is a good tool for teaching general relativity. Fig. 6 shows an example of a wormhole between the market place of Tübingen and a fictitious Mars station. Wormholes are typically visualized by drawings like Fig. 7, which could be considered an “industry standard” since they appear in practically every popular article on the subject. In fact, this kind of drawing probably gave wormholes their very name. While such an illustration is scientifically correct, it is nevertheless not sound because it gives the impression that a wormhole is a tube-like structure. In fact, a wormhole is not a tube, but a spherical object. Our visualization of the wormhole on the Tübingen market place (Fig. 6) comes much closer to giving this impression, especially if several pictures from several directions are presented or if an animated sequence can be

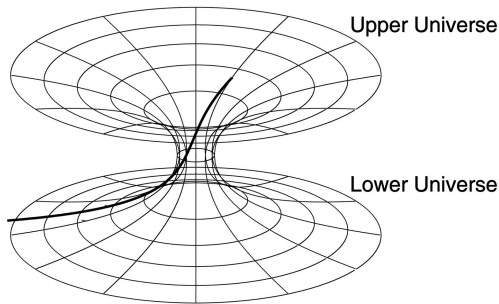


Fig. 7. A popular visualization of a wormhole that is scientifically correct, but nevertheless is not sound. © 2004 T. Müller.

shown. The unsound visualization of Fig. 7 does not show a wormhole in a (3+1)-D spacetime, but rather a (2+1)-D one, embedded in Euclidean space. Only the surface seen in the drawing comprises the wormhole, all the rest of the 3D space is not part of it. However, it involves a major step of mathematical abstraction to fully grasp this fact, even if it is carefully laid out in some accompanying text.

General relativistic ray tracing, as used for producing the egocentric visualizations in Fig. 4 and Fig. 6, tends to be several orders of magnitude slower than nonrelativistic ray tracing because of the significantly increased number of computations for constructing geodesic lines and intersecting polygonal rays with spacetime geometry. Therefore, parallelization is an urgent need for general relativistic ray tracing. Domain decomposition can be performed on the image plane because the computation of geodesics and ray-object intersections for one pixel is independent of those for other pixels. Good dynamic load balancing is achieved by choosing an appropriate granularity, which can be as fine as a single pixel. Parallel ray tracing scales well, even on distributed memory architectures with slow network connections, because only little communication is required between parallel computations. We regularly use a Linux cluster with 128 dual-processor nodes and Myrinet network connection. To give an impression of the rendering performance on our cluster computer: A $1,000^2$ image of a typical general relativistic scene takes about one to two hours on 28 nodes equipped with dual Pentium III (650 MHz) CPUs. The implementation of general relativistic ray tracing is based on *RayVis* [25], an object-oriented and extensible ray tracing program written in C++. Originally, *RayVis* was designed for nonrelativistic standard ray tracing. The aforementioned extensions have been included into the system by extending the functionality by subclassing.

4.3 Interactive Image-Based Gravitational Light Deflection

As shown above, interactive visualization of gravitational light bending is very challenging and impossible with today's and near-future low-cost hardware. Nevertheless, a few restricted, yet interesting scenarios can be visualized in real time. Several aspects have to be exploited simultaneously to achieve interactive visualization. First, only stationary scenarios in which scene objects are fixed and the metric is time-independent are considered. In this way, the representation of light rays and the intersection between rays and objects is reduced to three spatial dimensions.



Fig. 8. Museum installation for the visualization of gravitational light bending. A black hole serves as a gravitational source and can be interactively controlled by direct manipulation on the touch panel. The background image can be chosen from a collection of stored astronomical pictures or from real-time camera input (top-left part of the image).

Second, symmetric spacetimes are used to further decrease the number of independent dimensions. Third, the degrees of freedom for scene objects can be reduced. Fourth, visualization data can be partly precomputed and reused. Fifth, texturing capabilities of GPUs can be used to efficiently perform per-pixel computations.

We combine these aspects to reduce the visualization problem to computations on a 2D domain, which essentially results in image warping. In this way, efficient image-based general relativistic rendering is possible [26]. So far, we use two different spacetimes that facilitate image-based visualization: the Schwarzschild spacetime and the warp spacetime, which allows for faster-than-light travel [27]. This faster-than-light travel can be visualized as seen from the bridge of the warp spaceship by transforming a spherical panorama of objects that surround the spaceship at a sufficiently large distance, as detailed in our previous work [26].

We have recently implemented the real-time visualization of the Schwarzschild spacetime for interactive museum installations. Fig. 8 shows our installation for the exhibition in the "Stadthaus" in Ulm. The scenario contains a black hole, which serves as a gravitational source, and a background image, which is distorted due to gravitational light deflection. Because of the spherical symmetry of the Schwarzschild spacetime, the light rays starting at the camera exhibit cylindrical symmetry around an axis defined by the camera and the center of the black hole, i.e., it is sufficient to compute a 1D set of geodesic curves, described by the angle between light ray and symmetry axis. Moreover, the background geometry is assumed to be infinitely far away from the black hole so that, similarly to environment mapping, the direction of deflected light is sufficient to describe the intersection between light rays and background. Therefore, gravitational light bending leads to image deformations with cylindrical symmetry around the black hole. In our implementation, the CPU computes a 1D lookup table with deflection angles, which is used as a dependent texture to reconstruct the warping of the background by a GPU fragment program. Our OpenGL

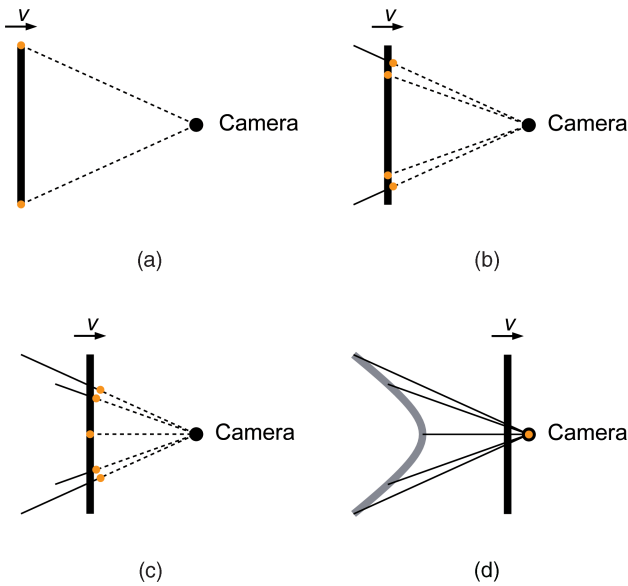


Fig. 9. Exocentric visualization of light propagation in a special relativistic setting. A rod is moving at constant speed to the right. The four images are snapshots of an animation that shows the position of the rod (thick vertical line) and the camera, as measured in the reference frame of the camera. Note that the measurement is performed simultaneously at different locations within the respective reference frame. Light propagation is illustrated for exemplary light rays: A thin, solid line indicates the distance covered by a light ray, an orange-colored dot marks the current position along a ray, a dashed line indicates the future positions. In image (d), the light rays are recorded at the same time by the camera, i.e., here the physical image construction takes place. By connecting the emission positions for the light rays, we can reconstruct the hyperbolic shape of the object as seen by the camera (thick light-gray line in image (d)). A related egocentric visualization is shown in Fig. 10. Based on a figure © 2002 U. Kraus.

GPU implementation on an ATI Radeon X800 XT GPU achieves some 70 fps for the simultaneous visualization on two output screens ($1,280 \times 768$ and $1,024 \times 768$), processing a $1,600 \times 1,200$ video input stream as background image in real time.

The user interface relies on direct manipulation. The black hole can be dragged on the touch-screen by using a finger, as shown in Fig. 8. At the lower part of the touch-screen, different background images can be chosen from a collection of stored astronomical pictures or from a camera covering the installation area. At the left part of the screen, the mass of the black hole can be modified by selecting different sizes of black hole icons. This restrictive and specialized interaction model is used to shift the flexibility-usability trade-off, inherent to any interactive system, toward high usability [28].

5 EXOCENTRIC ILLUSTRATION AND MULTICHANNEL VISUALIZATION

In addition to the egocentric visualization strategy, we selectively use exocentric approaches that are rooted in the tradition of mathematical visualization. An often-used type of exocentric visualization illustrates light propagation within special and general relativity from a third-person point of view. Fig. 9 shows a typical example for this kind of visualization. Here, a rod moves at constant speed toward

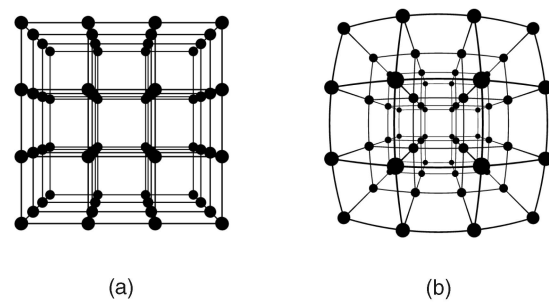


Fig. 10. Egocentric visualization of special relativistic motion of a cube-shaped lattice: (a) the lattice at rest and (b) the lattice approaching at $\beta = 0.9$. A related exocentric explanation of the hyperbolic shapes seen in the right image is given in Fig. 9. © 1999 D. Weiskopf.

the camera. This visualization is more abstract than the egocentric approach from Section 3 because of three reasons: 1) It shows positions of the rod as obtained from measurements, not through visual perception, 2) the pictures are not taken from the position of the camera, and 3) light propagation is shown as light-ray lines. Aspects 2) and 3) are not problematic with respect to the soundness of the visualization because similar abstractions are frequently used in many other illustrations so that the user is already familiar with them. Aspect 1) is more difficult because it involves the ability to distinguish between measurements (which are performed simultaneously at different locations within the same reference frame) and image generation (which is based on light that reaches the camera from the scene objects at the same time).

Therefore, such an exocentric visualization should be accompanied by some additional, explanatory text. Furthermore, we often combine egocentric visualizations with exocentric illustrations to achieve a multichannel visualization with tightly linked, separate views of the same scenario. Fig. 9 (exocentric) and Fig. 10 (egocentric) show a typical example. Through this combined presentation, the viewer can understand the apparent hyperbolic deformations of objects that are perpendicular to the direction of fast motion. Here, a sketchy “look-and-feel” is applied to the visual representation of both the egocentric and exocentric views, facilitating an easy mental connection between both views and emphasizing only the important visual elements. The implementation of this kind of exocentric view can reuse the algorithms for object-space special relativistic rendering (Section 3.1), which computes the same type of light paths.

We use a similar combined visualization of egocentric and exocentric views for other aspects of relativistic light propagation, including Lorentz contraction or time dilation within special relativity as well as gravitational light bending within general relativity. An example for the latter application is given in Fig. 5 and Fig. 8.

While the exocentric visualization of light rays is still very tightly related to the process of image synthesis, we have also explored more abstract visualizations. One example is a method for directly illustrating the concept of a curved space [29]. Traditionally, geometry is an important aspect of mathematical visualization [30], [31], [32]. Our approach is based on the principle of the Regge calculus, where a 4D curved spacetime is subdivided into

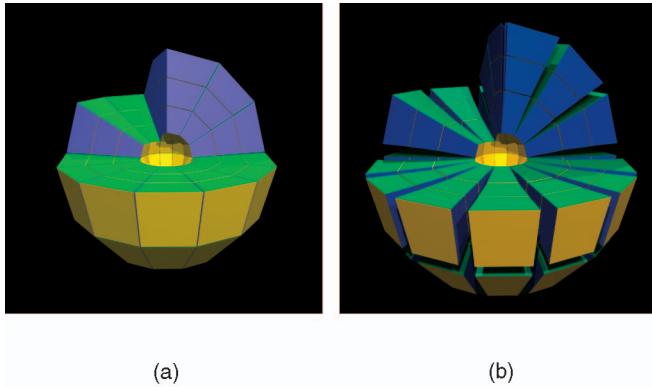


Fig. 11. Visualization of flat and curved spaces with building brick models: (a) flat (Euclidean) space and (b) curved space surrounding a black hole (inner boundary of the model at 1.25 Schwarzschild radii). © 2005 U. Kraus and C. Zahn.

small sections that are each intrinsically flat, similar to the approximation of a curved surface by small flat elements of surface area. Here, we confine ourselves to a space-like hypersurface of constant Schwarzschild time within Schwarzschild spacetime. This 3D space is subdivided into sections with intrinsic Euclidean geometry. The building bricks are assembled into a model that can be displayed in computer animations and can also be constructed as a paper model (see Fig. 11). Such a model is a 3D map of the space, computed to scale, and can be used, e.g., to determine geodesics (straight lines on the map) and the parallel transport of vectors (parallel lines on the map) by drawing on the model instead of solving differential equations. This permits a quantitative treatment of curved space, geodesics, and parallel transport on a high-school or undergraduate level where the analytic description of curved manifolds would be too advanced.

6 PLANETARY AND COSMOLOGICAL RENDERING

General relativity is the accepted theory of gravitation and, thus, the basis for cosmology. Therefore, the illustration of astronomical and cosmological aspects nicely comes along with relativistic visualization. Cosmology covers enormous time and length scales, which were, e.g., excellently visualized in the seminal film “Powers of Ten” [33]. More recently, Hanson et al. [34] have presented a truly large-scale visualization for cosmology, including the metaphor of the “cosmic clock,” which is used for their “Solar Journey” project [35]. Other related work deals with a sophisticated rendering of galaxies or nebulae [36], [37], [38].

In this section, we describe our visualization methods used in a film project for the exhibition in Bern. This film covers a time-lapse virtual journey from the Earth through the solar system, further away from our galaxy and, finally, to large-scale galaxy clusters. The main goal is to show the enormous length scales involved in astronomy and cosmology and, thus, physical correctness is most important, in particular, concerning the sizes of objects as well as their temporal and spatial relationships. Another goal is a visually aesthetic rendering that allows us to motivate museum visitors to view further, more complex visualizations of general relativity and cosmology.

The film production is decomposed in separate projects for planetary rendering and galaxy visualization. We start by discussing our tools for a virtual flight through the solar system. There already exist numerous and excellent tools for astronomical visualization and planet rendering (unlike the situation in relativistic visualization). We use “Celestia” [39] as the basis for planetary visualization because it is an extensible open-source tool with good visualization quality, excellent interactive camera navigation, and a physically correct modeling of both planetary and star constellations. We have slightly modified “Celestia” in three respects. First, antialiasing and motion blur have been included to improve image quality. Second, camera paths are interpolated with cubic or exponential splines, depending on the traversed length scale. Third, a file-based interface has been added to exchange camera paths with other tools.

Although “Celestia” is suitable for most parts of the journey through the solar system, it is not appropriate for close-by flights because extremely high-resolution terrain models are not supported. Therefore, we have developed a tool for high-quality and efficient planetary rendering with graphics hardware. Similarly to Cignoni et al. [40], who derive a planet-optimized version of their original BDAM terrain rendering method [41], we extend the terrain rendering software by Röttger et al. [42] for planetary visualization.

The original terrain rendering technique targets the visualization of DEM (digital elevation model) and color texture data defined on a flat uniform grid. Planetary terrain rendering essentially extends the domain from a planar surface to a spherical surface. Elevation data are interpreted as displacements along the normal vectors of the spherical domain. Spherical geometry has the problem that a global isometric mapping to a flat 2D texture is not possible. Therefore, the domain is typically split into several tiles that exhibit an almost uniform sampling rate for DEM and texture data. Tiling is realized by triangulating the boundaries between tiles, which may even have different resolutions of DEM and texture data. To save memory and reduce stress on the geometry pipeline of the GPU, an adaptive tessellation of the height field is employed. Following [42], we use a continuous level-of-detail of which the refinement criterion is governed by the distance of the viewer and a quality level. Temporal popping artifacts are eliminated by geomorphing, which smoothly interpolates between two neighboring resolution levels. Aliasing and flickering artifacts that may be caused by sampling of the surface texture are avoided by GPU-supported MIP mapping.

In addition to high-resolution terrain data, the most significant illumination aspects have to be considered to achieve a convincing and realistic visualization. Planets like the Earth or Mars have an atmosphere that greatly affects their appearance. Our starting point for atmospheric rendering is the model by Nishita et al. [43], who take into account Rayleigh and Mie scattering. By splitting the rendering process into a preprocessing and a GPU-based part, an interactive visualization is possible [44]. We adopt this rendering method and modify it in a few ways: The optical length lookup-table is enhanced so that it can be used for light attenuation between sample points and light

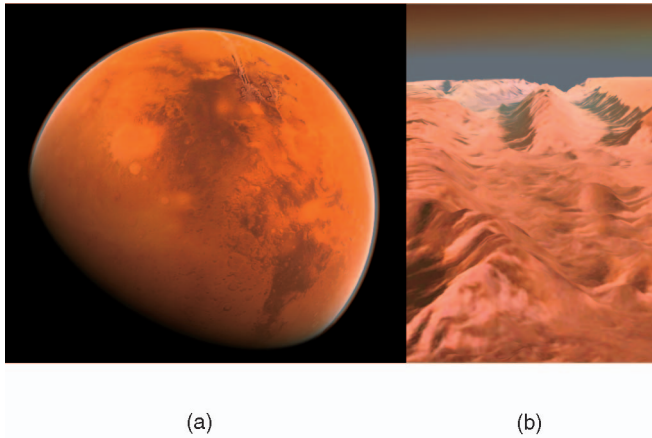


Fig. 12. Planetary terrain visualization of Mars, including atmospheric rendering: (a) outside view and (b) close-by flight.

source as well as between sample points and viewer. Attenuation is determined at runtime and mapped onto just two spheres. Therefore, we avoid lookups for shaded areas and expensive volume rendering for spherical layers.

Planetary rendering can be performed in real time if a low quality level is used. Interactive rendering is most useful for camera path planning. The final film rendering is done at high resolution, high quality level, and with time-consuming supersampling for spatial antialiasing and motion blur. Fig. 12 shows an example for Mars rendering, based on the MOLA terrain and texture data provided by NASA [45], with a resolution of $180 \times 360 \times 128^2$ floating-point elevation samples.

The other parts of the virtual cosmological journey require the rendering of objects like gas clouds, stars, or galaxies. Astronomical photographs or other 2D data sources are used as basis to construct 3D particle systems and fluids for Alias “Maya,” a commercial and generic modeling and animation tool, in order to model objects like the Horsehead Nebula, the distribution of cosmic background radiation, or quasars.

The complete film is composed from separate visualization sequences generated by the above tools. A consistent and smooth camera path is constructed by exchanging camera positions and orientations between different tools. Video editing is used to construct the final film.

7 VALIDATION AND EFFECTIVENESS

Our visualization activities can be validated from different points of view. A first category of goals can be classified as technical goals. Here, one objective is physical accuracy because our visualization strategy with egocentric views leads to realistic looking images that require accurate visual representation. This accuracy is achieved by applying numerical schemes with explicit error control to solve underlying physical simulations. Another objective is real-time capability for interactive visualizations. We achieve this goal by using efficient GPU implementations along with adaptive rendering methods. Third, stable and error-proof software is required for unsupervised interactive installations. Long-term installations in museum exhibitions, which

typically last for several months, have demonstrated the robustness of our software.

Another, even more important category of goals is concerned with the human recipients of visualization. Our objectives are to communicate phenomena of relativistic physics, to explain underlying concepts, and to motivate and inspire. Usually, the effectiveness of visualization is validated by user studies with controlled settings and a thorough statistical evaluation. This type of user study is not feasible for our visualizations because we address large groups of people with whom we have no, or only indirect and loose, contact. Therefore, a direct and controlled evaluation of the effects of visualization is difficult.

Nevertheless, we have considerable experience and manifold evidence for the effectiveness of our approach. One group of users are readers of popular science publications in magazines or books. We have no immediate contact with readers, but we can report on experiences with journalists, writers, and graphics designers who are responsible for preparing these publications. A general finding is that the egocentric strategy is strongly preferred by print media. Another observation is that familiar scenes are most popular—a large portion of our special relativistic visualizations for magazines shows high-speed travel through the Brandenburg Gate in Berlin, toward the Eiffel Tower in Paris, or around Saturn (the level of familiarity, of course, is dependent on the cultural background). Both observations show that visualizations with obvious implied information (i.e., natural egocentric visualization, mimicry based on well-known scenes) is most effective for publications that have to be concise because of limited printing space. A strong evidence for the effectiveness of our printed visualizations is a continuing media presence: Several popular science publications are carrying our visualizations. These magazines, such as “Bild der Wissenschaft,” “GEO Wissen,” or “Spektrum der Wissenschaft,” which is the German edition of “Scientific American,” typically have a number of printed copies in the range between 100,000 and 150,000 per issue. Our experiences with TV are very similar to those with print media; the same type of egocentric visualization is appropriate for films.

Oral presentations for a general audience are another environment in which visualization plays an important role. H. Ruder, a member of our research group, has extensive experience with invited talks on relativity and astrophysics; in 2004 and 2005 alone, he gave some 100 invited presentations for general audiences. The feedback from the audience is exclusively positive, even enthusiastic. Not only is the number of talks impressive, but also the number of people in the audience: On several occasions, talks were given to far more than a thousand people. H. Ruder was also awarded the most prestigious “Robert-Wichert-Pohl-Preis” by the “Deutsche Physikalische Gesellschaft” (German Physical Society, the world’s first and largest physical society) in 2002 for his excellence in communicating physics.

In addition, visualization is an important element in exhibitions. We have contributed to the scientific festival “Highlights der Physik” in Stuttgart (June 2004) and to exhibitions for the “Stadthaus” in Ulm (March 2004–August 2004), the “Historisches Museum” in Bern (June 2005–October 2006), and others. Visualization for museum exhibitions is distinct from those for popular science publications and invited talks. First, more in-depth information can be communicated to museum visitors, who

usually take more time for a museum visit than readers for a popular science article. In an exhibition, manifold information is presented which may range from historic background to most recent physical theories. Therefore, we are able to include not only egocentric visualizations, but also exocentric, mathematical visualizations. The latter are rather complex and need additional explanations, which are facilitated by another benefit of an exhibition: Several kinds of information can be shown simultaneously, e.g., an animated visualization can be displayed on a screen side-by-side with an accompanying explanation on a text panel and an additional still illustration, facilitating a multichannel visualization. Another difference is that interactive applications are possible. Interactive exploration leads to a better understanding than a fixed visualization because the user is actively involved. With large-screen displays and an appropriate user interface, even an impression of immersion can be achieved.

To give an example for feedback to exhibitions on Einstein and his theory of relativity, we provide some details about the exhibition in the "Historisches Museum" in Bern: In the first three months, some 100,000 visitors were counted with a record box-office result of \$1.4 million. According to P. Jezler, the museum director, the feedback from visitors is very positive—many people were so enthusiastic that they wanted to come back and see the exhibition again. He also reports that the average duration of a museum visit is slightly more than two hours and that most visitors view the video installations in full length. Due to the exhibition's success, it has been prolonged until October 2006, increasing its total length from 10 months to 16 months.

Finally, our illustrative visualizations have proven to be valuable teaching material. They provide a highly motivating introduction into the study of the theory of relativity. Apart from the fun aspect, they seriously assist teaching and learning. In teaching the theory of relativity, one must do without traditional classroom experiments. Visualization offers a substitute: "Experiments" can be performed with interactive visualization tools and "measurements" can be taken on paper model spacetimes. We make visualizations available to students and teachers (both high school and university teachers) by contributing regularly to physics teachers' continuing education seminars and to conferences on physics education. We have presented these projects in contributions to various teachers' journals and we also maintain a highly frequented Web site² on which we show images, movies, and explanatory texts on a level that is suitable for teaching at high school and introductory university level.

We refer to our project Web site³ for a detailed documentation of our visualization activities, including videos, further images, and extensive lists of diverse references.

8 CONCLUSION AND FUTURE WORK

We are convinced that visualization is a very useful tool for communicating and explaining complicated facts. We have successfully employed methods rooted in the tradition of scientific visualization in order to convey elements of the difficult theories of special and general relativity. We believe that illustrative visualization and visual communication should receive more attention by the scientific visualization community. Computer-based visualization has more to offer than exploration of data sets—it is capable of communicating physical phenomena or theoretical and mathematical concepts. After all, explanatory and illustrative visualization has a huge market of potential "customers," e.g., we have reached several million recipients with our images and films. We understand the term illustration in its broad and original sense,⁴ which includes the application of artistic drawing styles or traditional design (as in [47], [48], [49]), but also covers visual explanations.

From our experience, we think that the following aspects play an important role in explanatory visualization of relativity, but could also be valid for other applications.

First, domain knowledge is indispensable, which is in accordance with a long-standing demand in scientific visualization [50], [51]. We have included domain knowledge to a very large extent by teaming up experts in visualization, computer graphics, relativistic physics, physics education, modeling, and museum design.

Second, the facts implied in a visualization have to be taken into account. A good strategy is to reduce the amount and complexity of implied information by using simple and natural metaphors. We think that the approach of egocentric visual experiments, which can be regarded as a modification of the *Gedankenexperiments* (thought experiments) [8] frequently used by Einstein, is very successful. For interactive applications, in addition, the issue of the flexibility-usability trade-off should be considered. We recommend using highly specialized user interfaces with only a minimal choice of parameters. When more abstract visualizations are employed, they should be combined with additional (textual) information that explicitly states the connection between visual representation and displayed information. Furthermore, a multichannel visualization that combines egocentric visualizations with exocentric illustrations is useful for reducing interpretation problems associated with abstract presentations.

Third, the aesthetic-usability effect [52] is especially important for visual communication because attractive designs promote creative thinking and problem solving. Therefore, we use realistic looking, carefully designed models (e.g., Virtual Tübingen, 3D model of Bern), highly accurate measurements (e.g., MOLA Mars data), or image-based rendering with real-world data.

Fourth, the visualization workflow can usually be built upon a mix between standard off-the-shelf tools and individual developments. Standard tools have the obvious advantage of saving resources. For interactive visualization, however, custom-made software is often necessary. Our visualization methods benefit from the significant improvements graphics hardware has recently made. For example,

2. www.spacetime-travel.org (in English), www.tempolimit-lichtgeschwindigkeit.de (in German).

3. www.vis.uni-stuttgart.de/relativity.

4. Illustrate: to explain or decorate (a book, text, etc.) with pictures (from Collins English Dictionary [46]).

we have presented new GPU methods for image-based special relativistic rendering and interactive visualization of gravitational light deflection. Another reason for specific software development is that specialized visual mapping methods cannot be handled by existing tools. Examples are our extensions for 4D special relativistic ray tracing of accelerating scene objects, general relativistic ray tracing with multiple charts, and planetary-sized terrain rendering.

Fifth, the development of visualization contents is time-consuming because a good design typically requires many iterations. Thus, large visualization projects need good planning, a realistic timeline, and sufficient resources. For example, the exhibitions in Ulm and Bern required some two years of preparatory work.

For future work on the technical side, the performance of general relativistic visualization could be improved, e.g., by making use of intentional incompleteness or better numerical methods. On more fundamental grounds, it is a grand goal to find some kind of (formalized) metric to assess the effectiveness, soundness, and completeness of educational visualizations.

ACKNOWLEDGMENTS

This work was supported in part by SFU (start-up grant) and the "Deutsche Forschungsgemeinschaft" (SFB 382/D4). The authors thank H. Bühlhoff for his kind permission to use the 3D model of the "Virtual Tübingen" project [19], created at the Max Planck Institute for Biological Cybernetics, Tübingen. Special thanks to B.A. Salzer for proof-reading.

REFERENCES

- [1] T. Ertl, F. Geyer, H. Herold, U. Kraus, R. Niemeier, H.-P. Nollert, A. Rebetzky, H. Ruder, and G. Zeller, "Visualization in Astrophysics," *Proc. Eurographics*, pp. 149-158, 1989.
- [2] H.-P. Nollert, H. Ruder, H. Herold, and U. Kraus, "The Relativistic 'Looks' of a Neutron Star," *Astronomy and Astrophysics*, vol. 208, pp. 153-156, 1989.
- [3] D. Weiskopf, M. Borchers, T. Ertl, M. Falk, O. Fechtig, R. Frank, F. Grave, A. King, U. Kraus, T. Müller, H.-P. Nollert, I. Rica Mendez, H. Ruder, T. Schafhitzel, S. Schär, C. Zahn, and M. Zatloukal, "Visualization in the Einstein Year 2005: A Case Study on Explanatory and Illustrative Visualization of Relativity and Astrophysics," *Proc. IEEE Conf. Visualization*, pp. 583-590, 2005.
- [4] D.V. Black, "Visualization of Non-Intuitive Physical Phenomena," <http://www.hypervisualization.com>, 2005.
- [5] D. Weiskopf, "Visualization of Four-Dimensional Spacetimes," PhD thesis, Univ. of Tübingen, <http://w210.ub.uni-tuebingen.de/dbt/volltexte/2001/240>, 2001.
- [6] M.P. Consens, I.F. Cruz, and A.O. Mendelzon, "Visualizing Queries and Querying Visualizations," *SIGMOD Record*, vol. 21, no. 1, pp. 39-46, 1992.
- [7] J.D. Mackinlay, "Automatic Design of Graphical Presentations," Technical Report STAN-NCS-86-1138, Stanford Univ., Dept. of Computer Science, PhD thesis, 1986.
- [8] J.R. Brown, *The Laboratory of the Mind: Thought Experiments in the Natural Sciences*. London: Routledge, 1991.
- [9] D. Weiskopf, "Four-Dimensional Non-Linear Ray Tracing as a Visualization Tool for Gravitational Physics," *Proc. IEEE Conf. Visualization*, pp. 445-448, 2000.
- [10] C.W. Misner, K.S. Thorne, and J.A. Wheeler, *Gravitation*. New York: Freeman, 1973.
- [11] C. Møller, *The Theory of Relativity*, second ed. Oxford: Clarendon Press, 1972.
- [12] P.-K. Hsiung, R.H. Thibadeau, and M. Wu, "T-Buffer: Fast Visualization of Relativistic Effects in Spacetime," *Computer Graphics*, vol. 24, no. 2, pp. 83-88, 1990.
- [13] D. Weiskopf, D. Kobras, and H. Ruder, "Real-World Relativity: Image-Based Special Relativistic Visualization," *Proc. IEEE Conf. Visualization*, pp. 303-310, 2000.
- [14] E.H. Adelson and J.R. Bergen, "The Plenoptic Function and the Elements of Early Vision," *Computational Models of Visual Processing*, M. Landy and J.A. Movshon, eds., pp. 3-20, Cambridge: MIT Press, 1991.
- [15] P.-K. Hsiung and R.H.P. Dunn, "Visualizing Relativistic Effects in Spacetime," *Proc. Supercomputing Conf. '89*, pp. 597-606, 1989.
- [16] J. Li, H.-Y. Shum, and Q. Peng, "An Improved Spacetime Ray Tracing System for the Visualization of Relativistic Effects," *Proc. Eurographics 2001 Short Presentations*, 2001.
- [17] D. Weiskopf, "An Immersive Virtual Environment for Special Relativity," *Proc. Int'l Conf. Central Europe Computer Graphics, Visualization, and Computer Vision (WSCG '00)*, pp. 337-344, 2000.
- [18] D.A. Norman, *The Design of Everyday Things*. New York: Doubleday, 1990.
- [19] "Virtual Tübingen," <http://vr.tuebingen.mpg.de>, Max Planck Inst. for Biocybernetics, Tübingen, 2006.
- [20] S. Weinberg, *Gravitation and Cosmology: Principles and Applications of the General Theory of Relativity*. New York: John Wiley, 1972.
- [21] E. Gröller, "Nonlinear Ray Tracing: Visualizing Strange Worlds," *The Visual Computer*, vol. 11, no. 5, pp. 263-276, 1995.
- [22] D. Weiskopf, T. Schafhitzel, and T. Ertl, "GPU-Based Nonlinear Ray Tracing," *Computer Graphics Forum (Proc. Conf. Eurographics 2004)*, vol. 23, no. 3, pp. 625-633, 2004.
- [23] M.S. Morris and K.S. Thorne, "Wormholes in Spacetime and Their Use for Interstellar Travel: A Tool for Teaching General Relativity," *Am. J. Physics*, vol. 56, no. 5, pp. 395-412, 1988.
- [24] T. Müller, "Visual Appearance of a Morris-Thorne-Wormhole," *Am. J. Physics*, vol. 72, no. 8, pp. 1045-1050, 2004.
- [25] A. Gröne, "Entwurf eines objektorientierten Visualisierungssystems auf der Basis von Raytracing," PhD thesis, Univ. of Tübingen, 1996.
- [26] D. Kobras, D. Weiskopf, and H. Ruder, "General Relativistic Image-Based Rendering," *The Visual Computer*, vol. 18, no. 4, pp. 250-258, 2002.
- [27] M. Alcubierre, "The Warp Drive: Hyper-Fast Travel within General Relativity," *Classical and Quantum Gravity*, vol. 11, pp. L73-L77, 1994.
- [28] D.A. Norman, *The Invisible Computer: Why Good Products Can Fail, the Personal Computer Is So Complex, and Information Appliances Are the Solution*. Cambridge, Mass.: MIT Press, 1998.
- [29] U. Kraus and C. Zahn, "Wir basteln ein Schwarzes Loch—Unterrichtsmaterialien zur Allgemeinen Relativitätstheorie," *Praxis der Naturwissenschaften Physik*, vol. 54, no. 4, pp. 38-43, 2005.
- [30] K. Polthier, "Visualizing Mathematics—Online," *Mathematics and Art*, C.P. Bruter, ed., pp. 29-42, Berlin: Springer, 2002.
- [31] J. Weeks, "Real-Time Rendering in Curved Spaces," *IEEE Computer Graphics and Applications*, vol. 22, no. 6, pp. 90-99, Nov./Dec. 2002.
- [32] A.J. Hanson, T. Munzner, and G. Francis, "Interactive Methods for Visualizable Geometry," *Computer*, vol. 27, no. 7, pp. 73-83, July 1994.
- [33] C. Eames and R. Eames, "Powers of Ten," 9 1/2 minute film, 1977.
- [34] A.J. Hanson, C.-W. Fu, and E.A. Wernert, "Very Large Scale Visualization Methods for Astrophysical Data," *Proc. Eurographics/IEEE TCVG Symp. Visualization*, pp. 115-124, 2000.
- [35] A.J. Hanson, "Solar Journey Project," <http://www.cs.indiana.edu/~hanson>, 2006.
- [36] M. Magnor, G. Kindlmann, C. Hansen, and N. Duric, "Constrained Inverse Volume Rendering for Planetary Nebulae," *Proc. IEEE Conf. Visualization*, pp. 83-90, 2004.
- [37] M.A. Magnor, K. Hildebrand, A. Lintu, and A.J. Hanson, "Reflection Nebula Visualization," *Proc. IEEE Conf. Visualization*, pp. 255-262, 2005.
- [38] D.R. Nadeau, "Volume Scene Graphs," *Proc. Symp. Volume Visualization*, pp. 49-56, 2000.
- [39] "Celestia," <http://www.shatters.net/celestia>, 2006.
- [40] P. Cignoni, F. Ganovelli, E. Gobbetti, F. Marton, F. Ponchio, and R. Scopigno, "Planet-Sized Batched Dynamic Adaptive Meshes (P-BDAM)," *Proc. IEEE Conf. Visualization*, pp. 147-155, 2003.
- [41] P. Cignoni, F. Ganovelli, E. Gobbetti, F. Marton, F. Ponchio, and R. Scopigno, "BDAM—Batched Dynamic Adaptive Meshes for High Performance Terrain Visualization," *Computer Graphics Forum (Proc. Conf. Eurographics 2003)*, vol. 22, no. 3, pp. 505-514, 2003.

- [42] S. Röttger, W. Heidrich, P. Slusallek, and H.-P. Seidel, "Real-Time Generation of Continuous Levels of Detail for Height Fields," *Proc. Int'l Conf. Central Europe Computer Graphics, Visualization, and Computer Vision (WSCG '98)*, pp. 315-322, 1998.
- [43] T. Nishita, T. Sirai, K. Tadamura, and E. Nakamae, "Display of the Earth Taking into Account Atmospheric Scattering," *Proc. SIGGRAPH*, pp. 175-182, 1993.
- [44] Y. Dobashi, T. Yamamoto, and T. Nishita, "Interactive Rendering of Atmospheric Scattering Effects Using Graphics Hardware," *Proc. Conf. Graphics Hardware*, pp. 99-108, 2002.
- [45] "Mars Orbiter Laser Altimeter (MOLA) Science Investigation," <http://ltpwww.gsfc.nasa.gov/tharsis/mola.html>, NASA, 2006.
- [46] *Collins English Dictionary: Complete and Unabridged*, sixth ed. Glasgow: HarperCollins Publishers, 2004.
- [47] D. Ebert and P. Rheingans, "Volume Illustration: Non-Photorealistic Rendering of Volume Models," *Proc. IEEE Conf. Visualization*, pp. 195-202, 2000.
- [48] C.G. Healey, L. Tateosian, J.T. Enns, and M. Remple, "Perceptually Based Brush Strokes for Nonphotorealistic Visualization," *ACM Trans. Graphics*, vol. 23, no. 1, pp. 64-96, 2004.
- [49] D.H. Laidlaw, "Visualization Viewpoints: Loose, Artistic 'Textures' for Visualization," *IEEE Computer Graphics and Applications*, vol. 21, no. 2, pp. 6-9, Mar./Apr. 2001.
- [50] C. Johnson, "Top Scientific Visualization Research Problems," *IEEE Computer Graphics and Applications*, vol. 24, no. 4, pp. 13-17, July/Aug. 2004.
- [51] "Visualization in Scientific Computing," *Computer Graphics*, B.H. McCormick, T.A. DeFanti, and M.D. Brown, eds., vol. 21, no. 6, 1987.
- [52] M. Kurosu and K. Kashimura, "Apparent Usability vs. Inherent Usability: Experimental Analysis on the Determinants of the Apparent Usability," *Proc. ACM Conf. Human Factors in Computing Systems (CHI '95) Short Papers*, pp. 292-293, 1995.

The Team of Authors: The visualization activities described in this paper could only be accomplished by a large and interdisciplinary team of researchers, with expertise in relativistic physics, computer graphics, and physics education. Therefore, the authors come from a range of different institutions. Daniel Weiskopf is an assistant professor of computing science at Simon Fraser University. His research interests include scientific visualization and real-time computer graphics. Marc Borchers, Oliver Fechtig, Regine Frank, Frank Grave, Andreas King, Ute Kraus, Thomas Müller, Hans-Peter Nollert, Isabel Rica Mendez, Corvin Zahn, and Michael Zatloukal are with the Theoretical Astrophysics Group at the University of Tübingen, which is led by Hanns Ruder, who is a full professor of physics at the University of Tübingen. His group focuses primarily on research in astrophysics, general relativity, physics education, and biomechanics. Martin Falk and Tobias Schafhitzel are with the Institute of Visualization and Interactive Systems at the University of Stuttgart, which is led by Thomas Ertl, who is a full professor of computer science at the University of Stuttgart. The research at his institute focuses on scientific visualization and human-computer interfaces. Sonja Schär works at the Historisches Museum in Bern. She promotes the use of computer-based 3D modeling and animation for museum exhibitions.

► **For more information on this or any other computing topic, please visit our Digital Library at www.computer.org/publications/dlib.**